

Small-scale flows in SUMER and TRACE high-cadence co-observations[★]

M. S. Madjarska¹ and J. G. Doyle²

¹ Max-Planck-Institut für Sonnensystemforschung, Max-Planck-Str. 2, 37191 Katlenburg-Lindau, Germany
e-mail: madjarska@mps.mpg.de

² Armagh Observatory, College Hill, Armagh BT61 9DG, N. Ireland

Received 3 January 2008 / Accepted 14 February 2008

ABSTRACT

Context. We report on the physical properties of small-scale transient flows observed simultaneously at high cadence with the SUMER spectrometer and the TRACE imager in the plage area of an active region.

Aims. Our major objective is to provide a better understanding of the nature of transient phenomena in the solar atmosphere by using high-cadence imager and spectrometer co-observations at similar spatial and temporal resolution.

Methods. A sequence of TRACE Fe IX/X $\lambda 171$ Å and high-resolution MDI images were analysed together with simultaneously obtained SUMER observations in spectral lines covering a temperature range from 10 000 K to 1 MK.

Results. We reveal the existence of numerous transient flows in small-scale loops (up to 30 Mm) observed in the plage area of an active region. These flows have temperatures from 10 000 K (the low temperature limit of our observations) to 250 000 K. The coronal response of these features is uncertain due to a blending of the observed coronal line Mg X $\lambda 624.85$ Å. The duration of the events ranges from 60 s to 19 min depending on the loop size. Some of the flows reach supersonic velocities.

Conclusions. The Doppler shifts often associated with explosive events or bi-directional jets can actually be identified with flows (some of them reaching supersonic velocities) in small-scale loops. Additionally, we demonstrate how a line-of-sight effect can give misleading information on the nature of the observed phenomena if only either an imager or a spectrometer is used.

Key words. Sun: corona – Sun: transition region – line: profiles – methods: observational

1. Introduction

The solar atmosphere is highly dynamic on all scales seen both in spectroscopic and imager data. The dynamics is usually witnessed by non-Gaussian spectral line profiles, a strong radiance increase or proper motion of bright features (dark when seen in absorption). These events are commonly named transient phenomena due to their short duration. They have already been intensively studied for almost three decades during the High-Resolution Telescope and Spectrometer (HRTS), Yohkoh, Solar and Heliospheric Observatory (SoHO) and Transition Region And Coronal Explorer (TRACE) missions and it is strongly believed that they may contribute to both the coronal heating and solar wind generation. However, it is often difficult or even impossible to derive their spatial scale and even to identify their true nature because of the limitations of the existing instruments. Either high-cadence spectroscopic rastering, faster than the lifetime of these phenomena, or lower cadence rastering and simultaneous imaging can provide their correct identification and better understanding of the physical mechanisms involved.

Transient flows were studied since the Skylab mission (Mariska & Dowdy 1992) and later during the SoHO mission (for a recent overview see Doyle et al. 2006). Only recently a transient flow in a small-scale quiet-Sun loop was reported by Teriaca et al. (2004) detected in Solar Ultraviolet Measurement of Emitted Radiation (SUMER) data. The observations were taken in a very high-cadence rastering mode with 3 s exposure

time which permitted a “snapshot” of the area to be obtained. Transient flows in loops can be created by heating or pressure imbalance between the footpoints of a loop or by asymmetry in the footpoint areas (Boris & Mariska 1982; Spadaro et al. 1991; Orlando et al. 1995a,b). The heat deposition is believed to be located at the footpoints of the loop (Spadaro et al. 2006).

The phenomena which have all the characteristics of a transient feature are the so-called explosive events also known as bi-directional jets. They were seen both in the quiet Sun and active regions and were first observed with HRTS by Brueckner & Bartoe (1983) and later during the SoHO mission in SUMER observations (Innes et al. 1997). They are identified by their non-Gaussian profiles and were registered in spectral lines with formation temperatures from 4×10^4 K up to 6×10^5 K. No response was found so far at coronal temperatures (Teriaca et al. 2002). Their spatial size estimated from the appearance along a spectrometer slit is $3''$ – $5''$. Their lifetime ranges from 60 s to 300 s. Explosive events are mostly known from their spectral characteristics. Observations showing them simultaneously in imager and spectrometer data are very limited. Winebarger et al. (2001) used simultaneous TRACE and SUMER active region observations and found that short-term (≤ 5 min) intensity fluctuations in TRACE $\lambda 171$ Å data are on average 2.2 times larger in regions of reconnection than in a non-event region. The regions of reconnection were identified as the regions in which explosive event(s) were observed. The cadence of the TRACE observations was 50 s which is far too low to identify any proper motion if present. Innes (2001) made a detailed analysis of simultaneous SUMER Si IV $\lambda 1393$ Å line profiles, TRACE $\lambda 1550$ Å, $\lambda 1700$ Å

[★] An animation of the TRACE $\lambda 171$ Å images is only available in electronic form at <http://www.aanda.org>

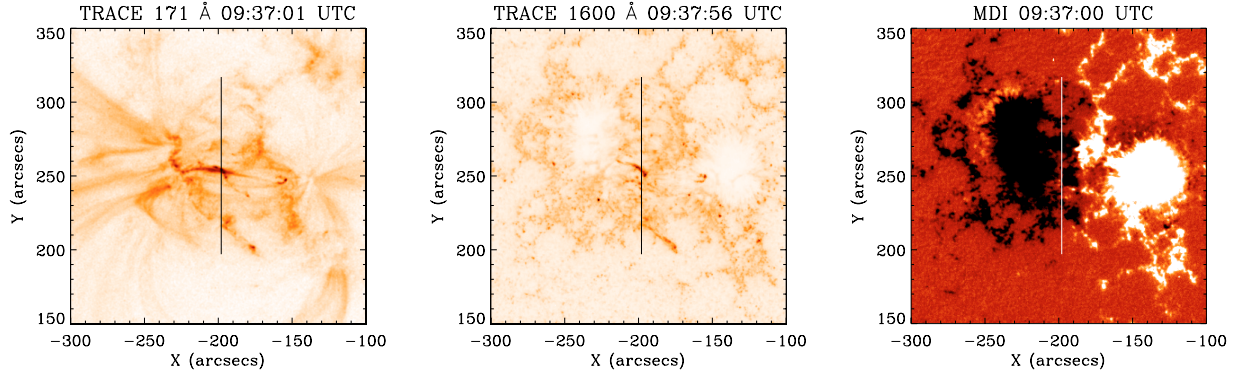


Fig. 1. Colour table reversed TRACE $\lambda 171$ Å (*left*) and TRACE $\lambda 1600$ Å (*middle*) images and MDI high-resolution magnetogram scaled from -200 to 200 G (*right*) of the active region NOAA 08558 observed on 1999 June 2 with the SUMER slit position over-plotted.

and $\lambda 171$ Å passband images and Michelson Doppler Imager (MDI) high-resolution magnetograms. The author found that in most events the Si IV $\lambda 1393$ Å line reveals plasma flows 1–2 min before the line core brightens suggesting that the plasma acceleration precedes plasma compression and/or heating.

The large variety of transient phenomena reported so far is mainly known from observations obtained with one particular instrument and in a certain wavelength range. We aim at studying in detail small-scale transients and determine their plasma and spatial characteristics using simultaneous spectroscopy and vacuum ultra-violet imaging at the highest existing spatial, temporal and spectral resolution (in the spectral range in question). We will also demonstrate the importance of having both imager as well as an imaging spectrometer data in order to avoid misinterpretation of an observed feature. In Sect. 2 we describe the observational material, its reduction and the way the co-alignment between the different instruments was done. Section 3 presents the data analysis, the obtained results and their discussion. In Sect. 4 we discuss the importance of multi-instrument observations. Conclusions as well as the future perspectives on the subject are given in Sect. 5.

2. Observations: SUMER, TRACE and MDI

The events discussed here occurred in the plage area of the active region NOAA 8558 on 1999 June 2 (Fig. 1). Simultaneous SUMER, TRACE and MDI observations were taken during several hours (see below for more details). The fields-of-views (FOVs) of SUMER, TRACE and MDI are shown in Fig. 1.

The SUMER spectrometer (Wilhelm et al. 1995; Lemaire et al. 1997) data ($1.5''$ spatial resolution) were taken on 1999 June 2 starting at 09:17 UTC and ending at 11:02 UTC. A slit with a size of $0.3'' \times 120''$ was used exposing for 25 s on detector B. The slit was pointed at the plage area of the active region between two sunspots of opposite polarities (Fig. 1). Four spectral windows were telemetered each with a size of 120 spatial \times 50 spectral pixels. The spectral line read-outs are shown in Table 1. From all lines only O V $\lambda 629.73$ Å was taken on the bare part of the detector. At the start of the observations the spectrometer was pointed at solar disk coordinates $x_{\text{cen}} = -217''$ (at 09:17 UTC) and $y_{\text{cen}} = 257''$. Subsequently, the observations were compensated for the solar rotation. The data were reduced using the standard procedures for flatfield, local gain and geometric distortion corrections. The spectral analysis was made with respect to a reference spectrum obtained by averaging over the entire dataset. We used the spectral atlas of Curdt et al. (2001), Sandlin et al. (1986) and Kelly (1987) to identify

Table 1. The observed spectral lines. The expression “/2” means that the spectral line was observed in second order. The comment “blend” means that the spectral line is blending a close-by line.

Ion	$\lambda/\text{Å}$	$\log(T)_{\text{max}}/\text{K}$	Comment
N V	1238.82	5.3	
C I	1248.00	4.0	
	1248.88		blend
C I	1249.00	4.0	
O IV/2	1249.24	5.2	blend
Si X/2	1249.40	6.1	blend
C I	1249.41	4.0	
Mg X/2	1249.90	6.1	
O IV/2	1250.25	5.2	blend
Si II	1250.09	4.1	
Si II	1250.41	4.1	
C I	1250.42	4.0	blend
S II	1250.58	4.2	
Si II	1251.16	4.1	
C I	1251.17	4.0	blend
Si V	1251.39	5.5	?
O IV/2	1251.70	5.2	
	1251.78		?
Si I	1258.78	4.1	
S II	1259.53	4.2	blend
O V/2	1259.54	5.4	
Si II	1260.44	4.1	

the spectral lines as well as cross-checking with the CHIANTI v5.2 database.

The TRACE (Handy et al. 1999) data were obtained in the Fe IX/X $\lambda 171$ and $\lambda 1600$ Å passbands starting at 09:00 UTC and finishing at 11:30 UTC on 1999 June 2. The integration time was 2.9 s for the $\lambda 171$ Å passband and 0.3 s for $\lambda 1600$ Å. The $\lambda 171$ Å channel cadence was 10 s which increased to 15 s when an image in the $\lambda 1600$ Å channel was taken. From 09:18:38 UTC until 09:32:28 UTC only observations in the $\lambda 1600$ Å channel were taken. The FOV of the images was $256'' \times 256''$ with a spatial resolution of $1''$. The most recent work on the TRACE $\lambda 171$ Å passband temperature response can be found in Brooks & Warren (2006).

The MDI (Scherrer et al. 1995) data were taken with a cadence of 1 min in high-resolution mode (pixel size $0.606''$) during several hours.

The co-alignment of TRACE and SUMER observations was done by using TRACE $\lambda 1600$ Å images and SUMER raster observations, taken just before the time series in the

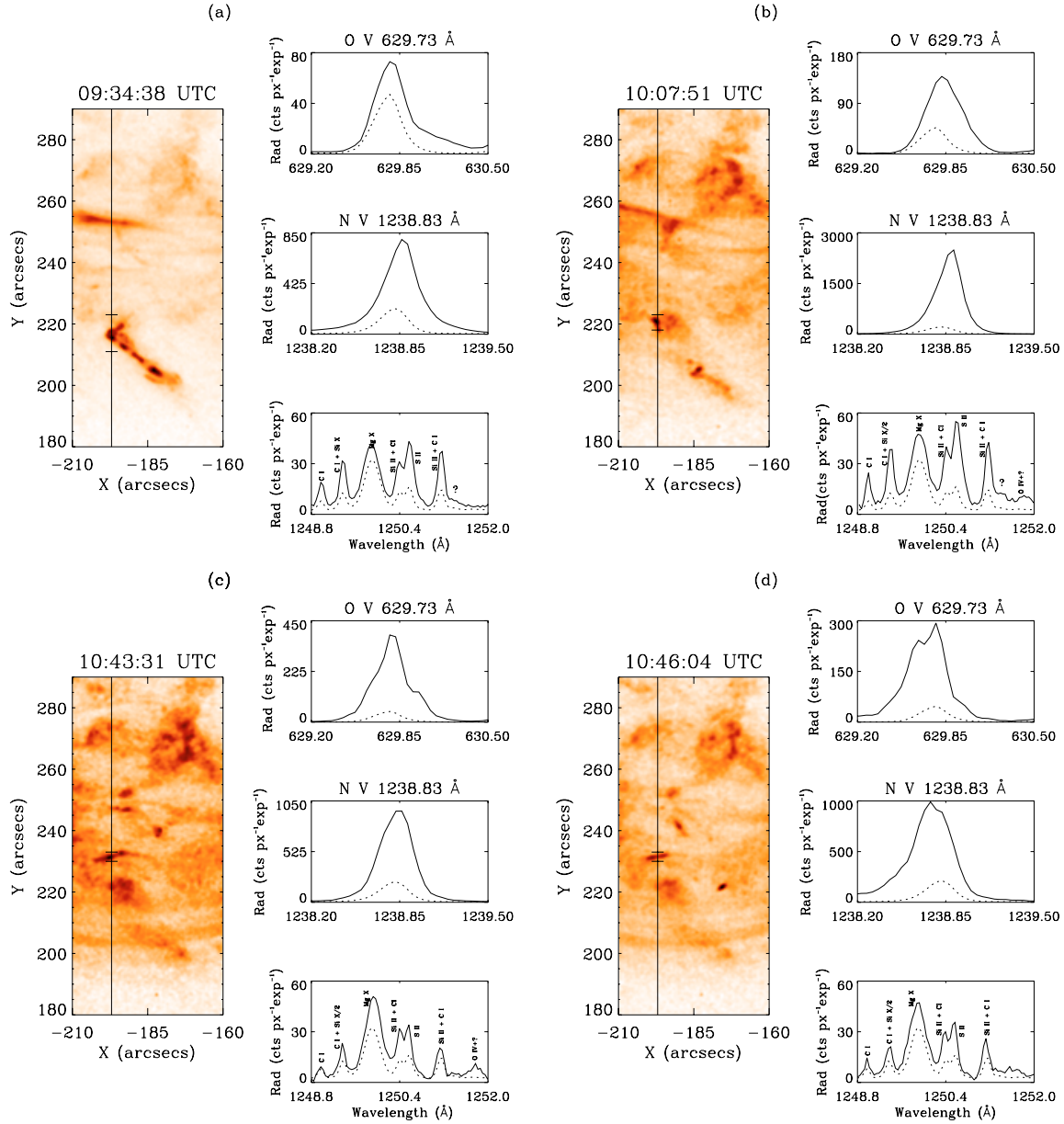


Fig. 2. For all cases **a**–**d**): *left*: TRACE $\lambda 171 \text{ \AA}$ colour table reversed image showing the analysed feature. The vertical line corresponds to the position of the SUMER slit, while the two horizontal lines outline the part of the slit which was analysed in the SUMER data. *right*: profiles of all observed spectral lines taken closest in time to the shown TRACE image. The dotted line profile corresponds to the reference spectrum. An animation of the TRACE $\lambda 171 \text{ \AA}$ images can be seen online.

Si II $\lambda 1260.44 \text{ \AA}$ ($\log T_{\max}/\text{K} = 4.1$) line which falls in the transmitted O V $\lambda 629.73 \text{ \AA}$ spectral window. The line formation temperatures are taken from CHIANTI v5.2 using the Mazzotta et al. (1998) ionisation equilibrium. The SUMER raster was obtained with 5 s exposure time and $0.37''$ increment. The emission in the TRACE $\lambda 1600 \text{ \AA}$ passband mainly comes from continuum emission, C IV, C I, and Fe II. Note that the SUMER times mark the beginning of the exposures, while the TRACE times mark the end of the exposures. The co-alignment between SUMER and MDI was done via the TRACE $\lambda 1600 \text{ \AA}$ channel. The precision of all co-alignments is $1''$.

3. Analysis and discussion of small-scale flows

The SUMER observations were taken in spectral lines with formation temperatures covering a temperature range from

10000 K to 1 MK. First, the two transition region lines O V $\lambda 629 \text{ \AA}$ and N V $\lambda 1238 \text{ \AA}$ were inspected for spectra showing non-Gaussian profiles or large intensity increases. That led to the identification of several events with profiles showing a radiance increase and either blue or/and red-shifted emission. The counterpart of these events in the TRACE $\lambda 171 \text{ \AA}$ images revealed several features of increased emission of circular shape with diameters of $3''$ and elliptical ones with major axis of $4''$ and minor axis of $2''$ along small-scale loops (length up to 30 Mm) (Fig. 2). This combined with the spectral information mentioned above led us to conclude that we actually observe plasma flows. The brightenings as seen in the TRACE images appear suddenly anywhere along the loops. We can only speculate that either the energy deposition happens at the position where first these brightenings are seen or simply due to higher density or filling factor that the plasma emits stronger in the

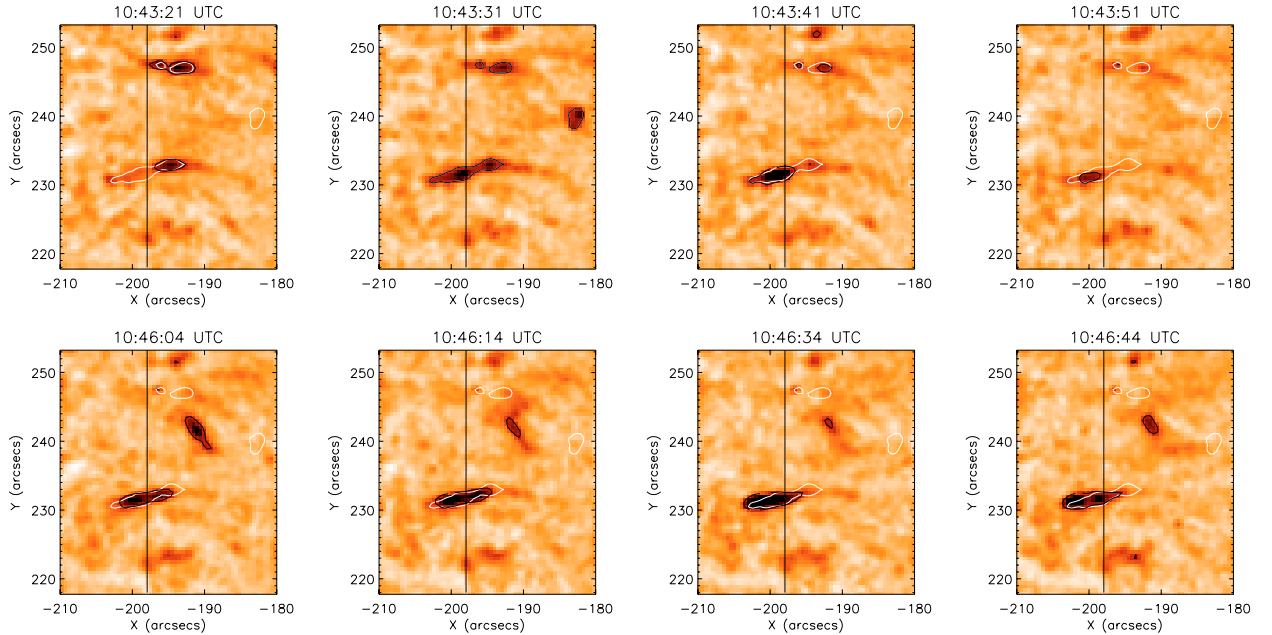


Fig. 3. TRACE $\lambda 171 \text{ \AA}$ colour table reversed image sequences of events (c) (above) and (d) (below). The black contour shows the brightening (here seen as the darkest feature) in the loop at a given time. The over-plotted white contour outlines the event at 10:43:31 UTC. The black contour traces the brightenings at the given time. The vertical line corresponds to the position of the SUMER slit.

TRACE $\lambda 171 \text{ \AA}$ channel at this place. We selected four events which were best registered with the two instruments both temporally and spatially. The transient flows have a different response in the registered spectral lines but nevertheless some common characteristics can be found.

Events (a) and (b) presented in Fig. 2 (top) both show a strong increase in the peak radiance of the rest component of N V of 3.5 and 12.5 times, respectively. The increase in the O V line is only a factor of 1.5 and 3.4. This is coupled with an average increase of 2.2 and 3.8 times in the chromospheric lines (C I, Si II and S II). How can we explain such a significant difference in the intensity flux increase of the two transition region lines O V and N V? One possible explanation is that although both lines have overlapping formation temperatures, their peak formation temperature is separated by $\Delta \log T_e = 0.08\text{--}0.12$ (depending on the assumed atomic model). A time dependent ionisation could also be an explanation which will be discussed in a forthcoming paper. Another possible reason was discussed by Doyle et al. (2005) where the authors derived the density dependent contribution function for both N V and O V. Their calculations showed that with increasing electron density, both lines shift towards lower temperatures. The difference comes, however, from the relative increase of the line flux with increasing density. For the N V line, increasing the density to 10^{11} cm^{-3} results in a 60% increase in the line flux, while the O V line shows a 30% decrease. Increasing the density to 10^{12} cm^{-3} results in a factor of two decrease of the O V flux.

Event (a) shows a Doppler shift of $80\text{--}90 \text{ km s}^{-1}$ in the red wing of the O V line and a rest component shifted at $\approx 5 \text{ km s}^{-1}$. For event (b) the rest component shift to the red in the O V line is $\approx 14 \text{ km s}^{-1}$ while the shift in the red wing of the line reaches up to 60 km s^{-1} . The Doppler shifts in O V were derived from a multi-Gauss fit.

The flows (c) and (d) cross the SUMER slit with a time difference of approximately 3 min. Using image difference techniques we found that these flows appear visibly at the same location, i.e. in the same loop (Fig. 2, bottom and Fig. 3). Visual in-

spection of the TRACE image sequence animation suggests that the plasma crossing the SUMER slit propagates in the same direction during both events. Despite moving along the same magnetic loop and in the same direction, there is quite a significant difference in the spectral line profiles during the two events. The Doppler shifts in the O V line (only for O V was it possible to apply a multi-Gauss fit) change from red (24 km s^{-1}) and blue-shift (50 km s^{-1}) for event (c) to a blue-shift of up to 45 km s^{-1} with a strong peak at 28 km s^{-1} and a red-shifted but not very intense component up to 38 km s^{-1} for event (d) (Figs. 3 and 4). What causes such a difference in the line profiles? One possible explanation is the line-of-sight effect created by the change of the orientation of the loop (due to, for instance, a footpoint displacement) in respect to the observer (SoHO/SUMER). We can only speculate that for case (c) the slit is closer to the top of the loop while for (d) the slit gets the emission more from the ascending plasma which produces the blue-shifted emission. As can be seen in Fig. 3, the projection of the flow on the TRACE images differs slightly for events (c) and (d). In fact, for these events, flows seems to propagate towards both footpoints of the loop when viewed with the TRACE images (only available in electronic form at www.aanda.org). The SUMER slit gets the emission only from one of them. A similar picture was also observed during other events registered in the TRACE field-of-view. However, we have to be cautious with the interpretation of what we see in the TRACE data, because without simultaneous spectral information we cannot be sure whether we observe a flow or simply a brightening.

Events (c) and (d) show a similar radiance increase which is stronger in the O V line (7.4 and 6.3 times with respect to the reference radiance, respectively) while the emission in N V increases only 4.6 and 4.3 times, respectively. This is coupled with a weaker response in the chromospheric lines with respect to events (a) and (b). It is therefore evident that a stronger response in the N V line is coupled with a stronger emission in the chromospheric lines (C I, Si II and S II).

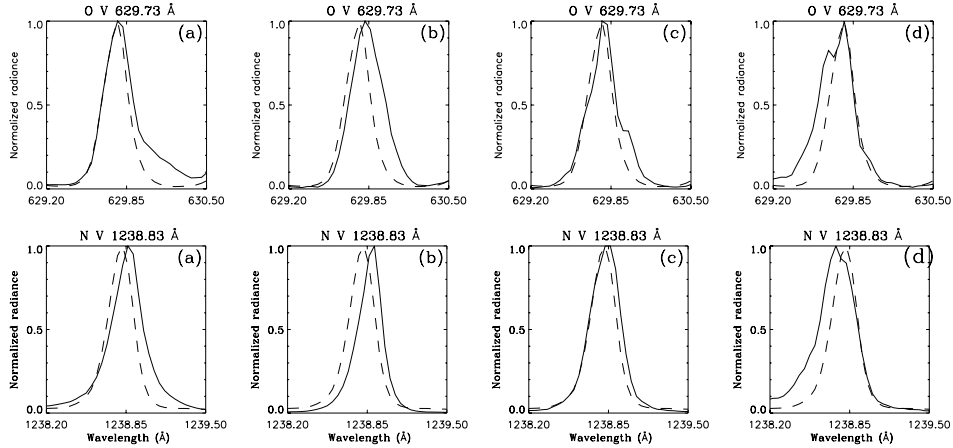


Fig. 4. Normalised O v and N v line profiles of the four events shown in Fig. 2. The dashed line is the reference spectrum.

Although there are some significant differences in the radiance increase of O v and N v, the Doppler shifts in the two transition region lines are almost the same for each transient (Fig. 4). If we assume that O v $\lambda 629 \text{ \AA}$ and N v $\lambda 1238 \text{ \AA}$ are in ionisation equilibrium they will emit at temperatures around 250 000 and 200 000 K which gives sound speeds of 75 km s^{-1} and 67 km s^{-1} , respectively. The fact that the flows direction forms an angle with respect to the line-of-sight means that some of these flows reach supersonic velocities.

The interpretation of the Mg x $\lambda 624.85 \text{ \AA}$ emission is complicated due to the fact that in the SUMER spectra this line when registered in second order is blended by several other lines including P II $\lambda 1249.82 \text{ \AA}$, Mg II $\lambda 1249.93 \text{ \AA}$, Si II $\lambda 1250.08 \text{ \AA}$ and O IV $\lambda 1250.25 \text{ \AA}$ in second order. Events (b), (c) and (d) show a significant increase in the feature at $\lambda 1249.90 \text{ \AA}$ but this is coupled with the presence of the O IV multiplet observed in second order (see Table 1 for details on these lines). Therefore, it remains uncertain whether these events reach coronal temperature, but equally we cannot reject such a possibility. Additionally, during some of the events, two spectral lines appear at around $\lambda 1251.39 \text{ \AA}$ and $\lambda 1251.70 \text{ \AA}$ blended with the O IV $\lambda 1251.70 \text{ \AA}$ indicated with a question mark on the spectra in Fig. 2. A possible candidate for the line at $\lambda 1251.39$ is Si v. This line has a very high excitation energy of the upper level, and therefore it can be excited only if the electron distribution function has an enhanced energy tail around $\log T/\text{K} = 5.2\text{--}5.5$ (Young, private communication). The second line at around $\lambda 1251.78 \text{ \AA}$ is not yet identified. Further work is needed regarding the identification of these lines.

The duration of the flows was determined from the time a brightening is first seen in the loop in the TRACE $\lambda 171 \text{ \AA}$ image until it disappears. The events last from 60 s in a very small loop (event (b)) up to 19 min (event (a)) for the largest loop. The duration in the SUMER data is based on the time the flow is seen crossing the slit and does not actually reflect the real lifetime of the events.

4. Line-of-sight effects revealed in imager and spectrometer co-observations

One of the aims of the present work is to show how a line-of-sight effect can give misleading information on the observed features when either only an imager or a spectrometer is used. In Fig. 5 a TRACE $\lambda 171 \text{ \AA}$ image illustrates a jet-like feature (for

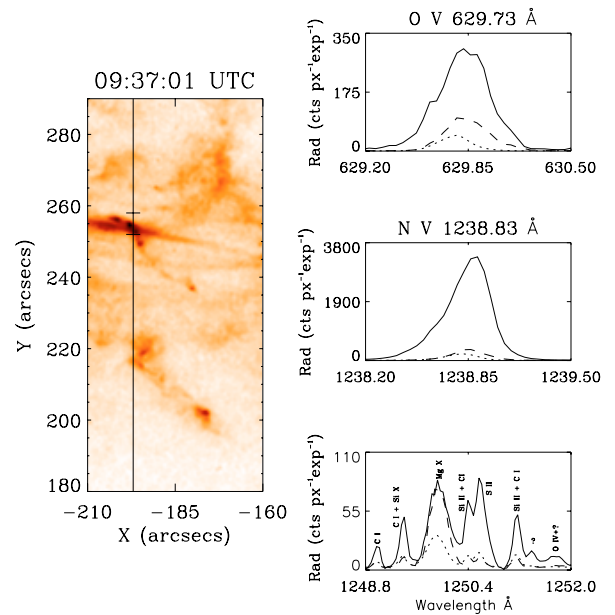


Fig. 5. *Left:* TRACE $\lambda 171 \text{ \AA}$ colour table reversed image showing the flow in a pre-existing coronal loop. The vertical line corresponds to the position of the SUMER slit, while the two horizontal lines outline the part of the slit which was analysed in the SUMER data. *Right:* a reference spectrum is shown with the dotted line. The dashed line corresponds to the spectrum registered at 09:22:17 UTC averaged over the area denoted by the two horizontal lines on the TRACE image. The continuous line is the spectrum around 09:37 UTC.

more details on this event see Madjarska et al. 2007) which is “crossed” by a blob-like flow along a loop (similar to the events discussed above). With imager information only, it would not be clear whether the two apparently crossing features are related to each other or not, and what their plasma characteristics are. Equally, the SUMER line profiles show a strong increase in all spectral lines in the transmitted spectral windows. As can be seen from Table 1 the spectral lines in question cover a temperature range from 10 000 K to 1 MK. The fact that we have both imaging and spectral information helps us to disentangle this puzzle. To find out the origin of the emission in each spectral line we took a spectrum obtained just before the blob flow was seen in the TRACE images. The corresponding profile at 09:22:17 UTC is shown with a dashed line in Fig. 5. This profile has only information from the jet-like feature. The comparison with the

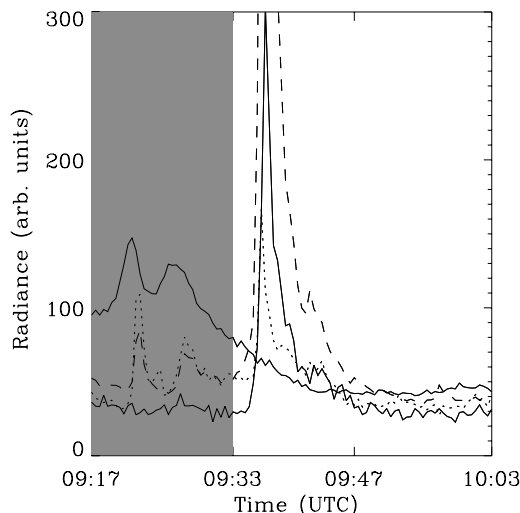


Fig. 6. The peak radiance averaged along the SUMER slit as shown in Fig. 5 obtained from a single Gauss fit. The solid line corresponds to the Mg X $\lambda 624.85$ Å line, dotted – O V $\lambda 629$ Å, dashed – N V $\lambda 1238$ Å, solid thick – Si II $\lambda 1251.16$ Å and C I $\lambda 1251.17$ Å. The grey area marks the time period during which the jet-like events were observed (see Madjarska et al. 2007).

reference spectrum (dotted line) and the spectrum (solid line) at 09:37:01 UTC (during the blob-like flow) shows that the emission in the Mg X line comes entirely from the jet-like event. A small amount of the O V emission belongs to the jet-like event (this is actually the fainting phase of the phenomenon, see Fig. 6) while the remaining emission belongs to the blob-like flow. The jet-like event as shown by Madjarska et al. (2007) emits only at coronal and transition region temperatures and no chromospheric emission was detected during the event(s). Therefore, the emission from the chromospheric lines belongs entirely to the blob-like flow. So, what we actually see in the TRACE 171 Å channel are two features happening at very different heights in the solar atmosphere which are not related to each other.

5. Conclusions

This paper presents a unique dataset which makes it possible to study features in the plage area of an active region using imager and spectrometer co-observations at the highest existing temporal, spectral (in the wavelength in question) and spatial resolution. We show that Doppler shifts often associated with explosive events or bi-directional jets can actually be identified with flows (some of them reaching supersonic velocities) in small-scale loops. We were able to determine the physical properties of these flows such as temperature, velocities, size and lifetime. The present results can add, however, very little on the understanding of the actual mechanism generating

these flows, but they can have a strong application for testing different models of generating plasma flows from any energy source like for instance magnetic reconnection. The present work will continue using data from Extreme-ultraviolet Imaging Spectrometer, X-ray Telescope and Solar Optical Telescope on board Hinode combined with data from already well known instruments such as SUMER, Coronal Diagnostic Spectrometer, MDI on SoHO and TRACE. Large datasets of simultaneous observations with the above mentioned instruments were acquired and preliminary work is ongoing. Hinode data should provide the answer to some of the open questions of the present work like for instance the coronal response to these transient phenomena.

We believe that with this work we were able to demonstrate that using simultaneous imager and spectrometer observations is of great importance for deriving correctly the plasma characteristics of the observed features and that this is one of the best ways to better understand the physical processes happening on the Sun.

Acknowledgements. We would like to thank W. Curdt for the fruitful discussions. We thank A. Theissen and D. E. Innes for the careful reading of the manuscript. SoHO is a mission of international co-operation between ESA and NASA. The SUMER project is financially supported by DRL, CNES, NASA, and PRODEX. Research at Armagh Observatory is grant-aided by the Northern Ireland Department of Culture, Arts and Leisure.

References

- Boris, J. P., & Mariska, J. T. 1982, *ApJ*, 258, L49
- Brooks, D. H., & Warren, H. P. 2006, *ApJS*, 164, 202
- Brueckner, G. E., & Bartoe, J.-D. F. 1983, *ApJ*, 272, 329
- Curdt, W., Brekke, P., Feldman, U., et al. 2001, *A&A*, 375, 591
- Doyle, J. G., Ishak, B., Ugarte-Urra, I., Bryans, P., & Summers, H. P. 2005, *A&A*, 439, 1183
- Doyle, J. G., Taroyan, Y., Ishak, B., Madjarska, M. S., & Bradshaw, S. J. 2006, *A&A*, 452, 1075
- Handy, B. N., Acton, L. W., Kankelborg, C. C., et al. 1999, *Sol. Phys.*, 187, 229
- Innes, D. E. 2001, *A&A*, 378, 1067
- Innes, D. E., Inhester, B., Axford, W. I., & Wilhelm, K. 1997, *Nature*, 386, 811
- Kelly, R. L. 1987, *Atomic and ionic spectrum lines below 2000 Angstroms. Hydrogen through Krypton* (New York: AIP, American Chemical Society and the National Bureau of Standards)
- Lemaire, P., Wilhelm, K., Curdt, W., et al. 1997, *Sol. Phys.*, 170, 105
- Madjarska, M. S., Doyle, J. G., Innes, D. E., & Curdt, W. 2007, *ApJ*, 670, L57
- Mariska, J. T., & Dowdy, Jr., J. F. 1992, *ApJ*, 401, 754
- Mazzotta, P., Mazzitelli, G., Colafrancesco, S., & Vittorio, N. 1998, *A&AS*, 133, 403
- Orlando, S., Peres, G., & Serio, S. 1995a, *A&A*, 294, 861
- Orlando, S., Peres, G., & Serio, S. 1995b, *A&A*, 300, 549
- Sandlin, G. D., Bartoe, J.-D. F., Brueckner, G. E., Tousey, R., & Vanhoosier, M. E. 1986, *ApJS*, 61, 801
- Scherrer, P. H., Bogart, R. S., Bush, R. I., et al. 1995, *Sol. Phys.*, 162, 129
- Spadaro, D., Antiochos, S. K., & Mariska, J. T. 1991, *ApJ*, 382, 338
- Spadaro, D., Lanza, A. F., Karpen, J. T., & Antiochos, S. K. 2006, *ApJ*, 642, 579
- Teriaca, L., Banerjee, D., Falchi, A., Doyle, J. G., & Madjarska, M. S. 2004, *A&A*, 427, 1065
- Teriaca, L., Madjarska, M. S., & Doyle, J. G. 2002, *A&A*, 392, 309
- Wilhelm, K., Curdt, W., Marsch, E., et al. 1995, *Sol. Phys.*, 162, 189
- Winebarger, A. R., DeLuca, E. E., & Golub, L. 2001, *ApJ*, 553, L81